Drug Design, Development and Therapy

Dovepress
Taylor & Francis Group

Open Access Full Text Article

ORIGINAL RESEARCH

The Potential Mechanisms of *Althaea rosea* (Linn.) Cavan. Flower in Alleviating Tetrodotoxin Poisoning: An Integrated Metabolomics, Network Pharmacology and Experimental Validation

Renjin Zheng[1,2], Youjia Wu[1], Lingyi Huang[1], Fanxiang Zeng[3], Liying Huang[1]

[1]School of Pharmacy, Fujian Medical University, Fuzhou, Fujian, 350122, People's Republic of China; [2]Physical and Chemical Analysis Department, Fujian Center for Disease Control and Prevention, Fujian Provincial Key Laboratory of Zoonosis Research, Fuzhou, Fujian, 350012, People's Republic of China; [3]Department of Pharmacy, Fujian Maternity and Child Health Hospital; China Fujian Key Laboratory of Women and Children's Critical Diseases Research [Fujian Maternity and Child Health Hospital (Fujian Women and Children's Hospital)], Fuzhou, Fujian, 350001, People's Republic of China

Correspondence: Liying Huang; Fanxiang Zeng, Email fjmuhly88@sina.com; funshungceng@163.com

Purpose: Tetrodotoxin (TTX) poisoning manifests rapidly and severely, and there are currently no clinically effective treatments. *Althaea rosea* (Linn.) Cavan. flower, documented in the "National Compendium of Chinese Herbal Medicines", is traditionally recognized and clinically applied for its potential to mitigate tetrodotoxin (TTX) poisoning. This study aims to explores the pharmacodynamic components and mechanisms of the ethyl acetate extract of *Althaea rosea* flower (EAEAR) in a TTX-induced rat model.

Methods: Ultra-performance liquid chromatography coupled with quadrupole Orbitrap high-resolution mass spectrometry (UPLC-Q-Orbitrap-HRMS) was used to identify active components in EAEAR. Metabolomics combined with network pharmacology was used to explore the mechanisms underlying the mitigating effects of EAEAR in TTX-intoxicated rats. Experimental validation was performed on key targets of the pathway through Western blotting or enzyme-linked immunosorbent assay. And differential metabolites in key pathways were further validated using ultra-performance liquid chromatography coupled with triple quadrupole tandem mass spectrometry (UPLC-QqQ-MS/MS).

Results: A total of 35 active components were identified in EAEAR, 12 core components and 15 core targets were screened in network pharmacology, and metabolomics revealed 15 different metabolites. The arginine and proline metabolism pathway and the arginine biosynthesis pathway were identified as critical pathways for EAEAR's effect in alleviating TTX poisoning. Validation results indicated that EAEAR treatment led to significant alterations (P <0.05) in six key targets (MAOA, AOC1, ALDH7A1, NAGS, NOS2, and NOS3) and three differential metabolites (GABA, Pro, and NAG) in TTX-intoxicated rats.

Conclusion: EAEAR alleviates TTX poisoning symptoms by modulating targets and metabolites in the arginine and proline metabolism pathways and the arginine biosynthesis pathway. This study provides a theoretical basis for further exploration of its therapeutic potential and mechanisms against TTX poisoning.

Keywords: *Althaea rosea* (Linn.) Cavan. flower, tetrodotoxin, active component, detoxication, metabolomics, network pharmacology

Introduction

Tetrodotoxin (TTX) is a highly toxic neurotoxin with an acute reference dose of 0.25 μg/kg body weight set by the European Food Safety Authority.[1] TTX selectively binds to voltage-gated sodium channels (VGSCs) on neuronal cells, specifically targeting the highly conserved pore region (P-loop) of VGSCs.[2] By binding to amino acid residues near the α-subunit of the VGSC pore, TTX blocks the entry of Na^+ ions into the cell, leading to the depolarization of action potentials and impaired conduction in neurons, which result in paralysis of the peripheral and central nervous systems, potentially causing severe muscle paralysis and even death.[3] TTX is not only found in pufferfish but also in certain

Received: 8 November 2024
Accepted: 29 March 2025
Published: 5 May 2025

Graphical Abstract

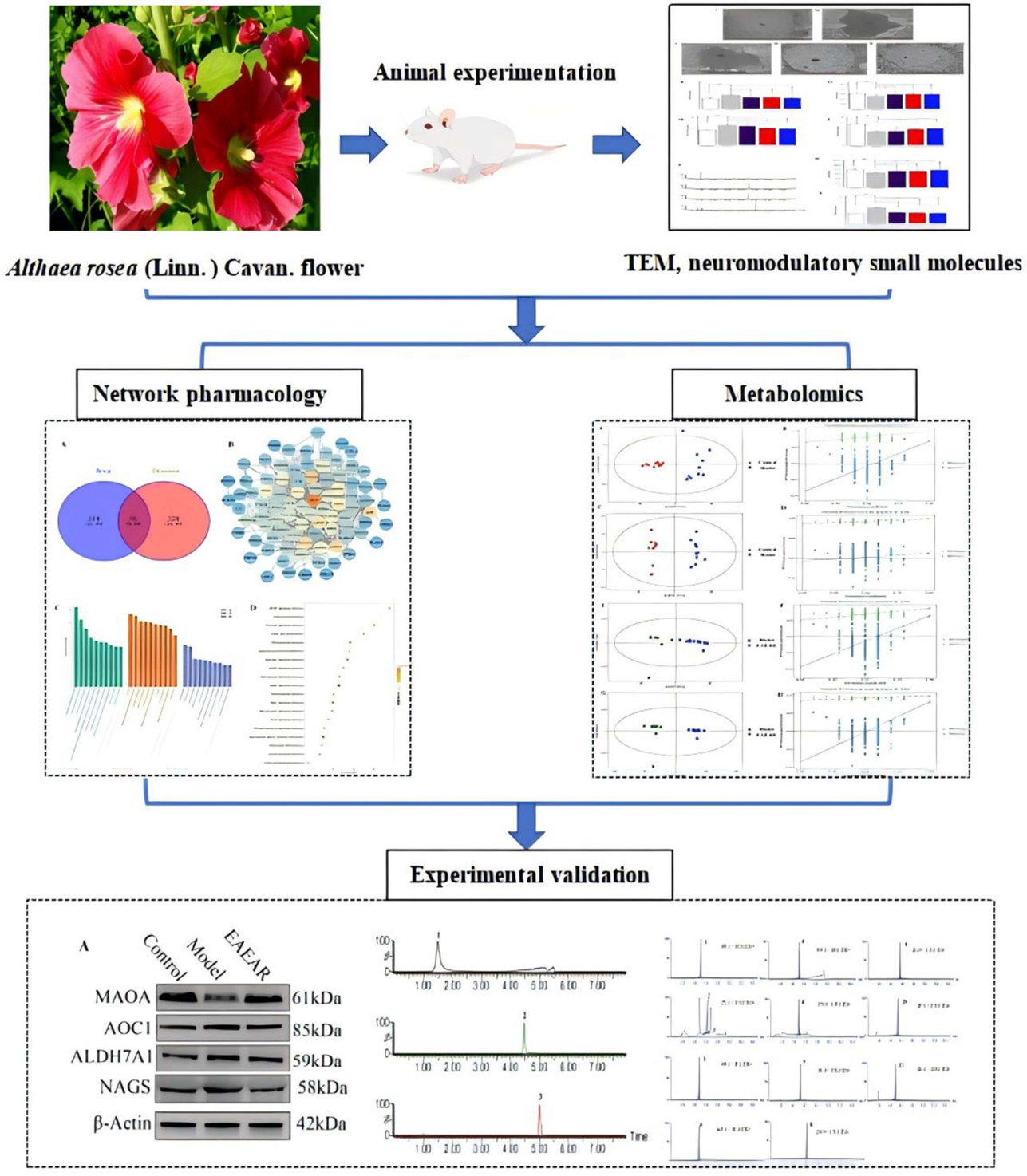

 https://doi.org/10.2147/DDDT.S505270

gastropods, cephalopods, and *bivalves*.[4,5] The occurrence of poisoning incidents due to the accidental consumption of TTX-contaminated seafood poses a serious threat to public health.[6] However, no specific antidotes for TTX are currently available, and the need for the development of effective therapeutic agents for TTX poisoning in clinical settings is urgent.

The *Althaea rosea* (Linn.) Cavan. flower (*Althaea rosea* flower), which belongs to the Malvaceae family and the genus Althaea, is a traditional Chinese medicinal herb (Supplementary Figure 1). According to the "National Compendium of Chinese Herbal Medicines", the *Althaea rosea* flower is known for its detoxifying and dispersing properties and is specifically mentioned for its ability to counteract TTX poisoning.[7] In a clinical study by Liu et al[8] through the use of *Althaea rosea* flowers to treat patients with TTX poisoning, the treatment group had a significantly shorter average hospital stay and faster symptom relief than the control group ($P < 0.05$). Wang et al[9] conducted a study in which 60 patients with TTX poisoning were randomly divided into a control group receiving standard symptomatic Western medical treatment and a treatment group receiving *Althaea rosea* flower as an adjunct therapy. The study found that the cure rate in the *Althaea rosea* treatment group significantly increased from 60% to 90% compared with the control group ($P < 0.05$).

Although the "National Compendium of Chinese Herbal Medicines" records that *Althaea rosea* flower can alleviate TTX poisoning, and clinical studies have demonstrated its therapeutic effects, the bioactive components and mechanisms underlying its efficacy remain unclear due to the complex and diverse chemical composition of the *Althaea rosea* flower. Metabolomics, focusing on subtle changes in endogenous small molecule metabolites in organisms under external stimuli or disease conditions, is widely applied in pharmaceutical research to reveal information on metabolic changes following drug intervention.[10] Network pharmacology explores the interaction networks between drugs and target proteins, predicting potential targets and pathways affected by the drug.[11] Integrating metabolomics and network pharmacology offers a multifaceted approach to uncovering the mechanisms and interactions of traditional Chinese medicine in disease treatment.[12]

This study successfully identified 35 active components in the ethyl acetate extract of *Althaea rosea* flower (EAEAR) using ultraperformance liquid chromatography–quadrupole–orbitrap high-resolution mass spectrometry (UPLC-Q-Orbitrap-HRMS). A TTX poisoning rat model was established, and a comprehensive exploration of the ameliorative effects of EAEAR on TTX poisoning was conducted through metabolomics, network pharmacology, and experimental validation of key targets in relevant pathways. This study reveals the active components and mechanisms by which *Althaea rosea* flower alleviates TTX toxicity. The application of modern pharmacological multiomics strategies to traditional Chinese medicine in this research provides new strategies and theoretical foundations for developing drugs to treat TTX poisoning.

Materials and Methods

Reagents and Materials

The herbal material was purchased from the Ximen Herbal Market in Fuzhou, Fujian Province, China, and it was authenticated as the dried flowers of *Althaea rosea* (Linn.) Cavan. by experts from the Department of Natural Medicinal Chemistry at Fujian Medical University. The herbarium sample is stored in Room 309, South Building of the School of Pharmacy, Fujian Medical University.

TTX (purity ≥ 98%, A170412) was acquired from Beijing Meizheng Bio-Tech Co., Ltd.; 4-Aminobutyric acid (GABA, purity ≥ 99%,1ST1403), L-Proline (Pro, purity ≥ 98%, 1ST2074), N-Acetyl-L-phenylalanine (N-Ac-L-Phe, purity ≥ 99.9%, 1ST2368), L-Acetylcarnitine (ALCAR, purity ≥ 98%, 1ST2381), and N-Acetyl-L-glutamic acid (NAG, purity ≥ 99%, 1ST2074) were acquired from Tianjin Alta Technology Co. Ltd.; Superoxide dismutase (SOD, A001-1) assay kit and malondialdehyde (MDA, A003-1) assay kit were supplied from Nanjing Jiancheng Bioengineering Institute; β-Actin (GB15001) was acquired from Wuhan Servicebio Technology Co. Ltd., China; N-acetylglutamate synthase (NAGS, 21566-1-AP) was sourced from Wuhan Sanying Biotechnology, China; Amine oxidase copper containing 1 (AOC1, CQA1314) was gained from Suzhou Cohesion Biosciences, China; monoamine oxidase A (MAOA, YT2635) and aldehyde dehydrogenase 7 family member A1 (ALDH7A1, YT6728) were supplied from Beijing

ImmunoWay Biotechnology, China; inducible nitric oxide synthase 2 (NOS2, E-EL-R0520c). ELISA kit and endothelial nitric oxide synthase 3 (NOS3, E-EL-R0367c) were acquired from Wuhan EIAab Science Co. Ltd., China.

Preparation of the EAEAR

According to the group's previous research,[13] EAEAR was found to have an interventional effect on TTX-intoxicated rats. The brief steps for the preparation of EAEAR, as described in the literature,[14] are as follows: Approximately 5 kg of dried *Althaea rosea* flowers were mechanically crushed and extracted twice with 10 times the volume of 95% ethanol by heating under reflux for 2 h each time. The two filtrates were combined, and the ethanol was removed by rotary evaporation under reduced pressure to obtain a concentrated extract, which was then vacuum-dried for 4 h to give a dark purple alcoholic extract. The resulting extract was dispersed in an appropriate amount of warm water (60 °C) and subsequently extracted three times with ethyl acetate. The combined ethyl acetate extracts were concentrated by rotary evaporation to near dryness and then redissolved in a suitable amount of deionized water. The solution was frozen at − 20 °C and lyophilized twice, yielding a lyophilized powder of EAEAR with a yield of 0.72%.

Animals and Treatments

Animal Modeling and Dosing Regimens

Specific pathogen-free (SPF) male Wistar rats were purchased from Shanghai Slack Laboratory Animal Co. Ltd. (Animal Production License No.: SCXK (Hu) 2022–0004). Rats weighing 145–155 g were used for the experiment and were quarantined within 3 days from the date of purchase. They were then allowed to adapt for one week before the experiment, with free access to food and water. The laboratory environment was maintained at a temperature of (23 ± 1) °C, a relative humidity of (50 ± 10)%, and a 12h light-dark cycle. The rats were housed in the barrier environment of the SPF-level laboratory animal facility at Fujian Medical University (Use License No. SYXK [Min] 2022–0003). All animal experiments were approved by the Ethics Committee of Fujian Medical University (Project Ethics No. FJMU IACUC 2022–0492) in accordance with the guidelines for animal experimentation for animal experimentation provided by the National Science and Technology Ethics Committee of China.

The 50 male SPF grade Wistar rats were randomly divided into five groups, with 10 rats in each group: control group, TTX intoxication model group (Model), TTX+ low dose EAEAR treatment group (EAEAR-L), TTX+medium dose EAEAR treatment group (EAEAR-M), and TTX+high dose EAEAR treatment group (EAEAR-H). Except for the control group, which received an intramuscular injection of 0.0035% citric acid, the other groups received a single intramuscular injection of TTX (11.75 μg/kg·bw) to establish the TTX intoxication model, with an injection volume of 1 mL/kg.bw.[13] After TTX intoxication, EAEAR was administered orally to the treatment groups at different doses: 11.25, 22.5, and 45.0 g/kg. The EAEAR dose of 22.5 g/kg was based on a previous study in which adults were treated orally with 500g fresh *Althaea rosea* flower decoction orally,[15] and then the equivalent dose was calculated according to the rules of dose conversion between humans and experimental animals, ie the EAEAR-M dose group. The low (EAEAR-L), and high (EAEAR-H) doses were half or twice the equivalent dose, respectively, allowing us to assess the dependence between efficacy and dose and to determine the optimal therapeutic dose for the treatment of TTX poisoning. Physiological saline (0.9% NaCl) was used as the solvent to prepare the EAEAR doses for administration to the animals. for EAEAR-L, EAEAR-M, and EAEAR-H groups, respectively. Treatments were administered once daily for 7 consecutive days. The control and model groups received saline by gavage at a dose of 10 mL/kg.

Sample Collection and Processing

Collection of serum samples: After the last dose, the rats were fasted for 12 h with free access to water. Blood samples were collected via tail vein puncture and were centrifuged at 3,000 rpm for 10 minutes at 4 °C. The supernatant was carefully aliquoted to obtain the serum samples, which were subsequently stored at −80 °C for biochemical assays and neuroregulatory small molecule analysis.

Collection of cerebral cortex: Portions of the motor cortex were fixed with 4% paraformaldehyde for Nissl staining and optical microscopy and in with 2.5% glutaraldehyde for transmission electron microscopy. The remaining cerebral cortex samples were stored at −80 °C for further analysis.

Oxidative Stress Analysis

Serum samples were removed from the refrigerator, allowed to stand at room temperature, and then assayed for the biochemical indicators SOD and MDA by enzyme-linked immunosorbent assay (ELISA) according to the kit instructions.

Neuromodulatory Small Molecule Analysis

Preparation of standard solutions for neuromodulatory molecules: The following were precisely weighed: 10.00 mg each of 4-aminobutyric acid, L-proline, N-acetyl-L-phenylalanine, and L-acetylcarnitine standards, and they were dissolved in water to make it up to 10 mL in a volumetric flask to prepare stock standard solutions at a concentration of 1.000 mg/mL. The stock solutions were stored at 4 °C. The intermediate mixed standard solution was prepared by accurately pipetting 1 mL of each stock solution and diluting with purified water to a final volume of 100 mL, resulting in a concentration of 10.00 μg/mL. This intermediate solution was stored at 4 °C. Before use, the intermediate solution was further diluted with purified water to prepare a series of mixed working solutions for the standard curve.

Chromatographic conditions: Chromatographic separation was conducted on a Tosoh TSK-Gel Amide-80 column (5 μm, 2.0 mm × 150 mm). The mobile phase consisted of 0.1% formic acid in water (A) and acetonitrile (B), with gradient elution as follows: 0–2 min, 15% A; 2–6 min, 15–85% A; 6–6.5 min, 85% A; 6.5–7 min, 85–15% A; 7–8 min, 15% A. The flow rate was 0.35 mL/min, with an injection volume of 5 μL and a column temperature of 30 °C.

Mass spectrometry conditions: The analysis was performed using a Xevo TQ-XS/Acquity UPLC I-Class system (Waters Corporation, USA) with multiple reaction monitoring (MRM) mode. The ionization was achieved using an electrospray ionization (ESI) source, operating in positive and negative ion modes. The capillary voltage was set at 3.0 kV, the ion source temperature was 150 °C, the desolvation temperature was 500 °C, and the desolvation gas flow rate was 800 L/hr.

Rat serum sample preparation: Approximately 100 μL of rat serum was taken, and 300 μL of acetonitrile was added to precipitate proteins. Vortexing was conducted for 1 min, and then centrifugation followed at 14,000 rpm for 10 min. The supernatant was filtered through a 0.22 μm PTFE membrane and used for injection.

Histopathological Analysis

Small pieces of the mouse cerebral cortex tissue (approximately 1 mm × 1 mm × 1 mm) were rapidly immersed in a 4 °C fixative solution for 2–4 h, followed by rinsing with 0.1 mol/L phosphate buffer. The tissue was then fixed with 1% osmium acid for 2 h at room temperature and rinsed again. Tissue samples were then dehydrated through a graded series of ethanol and acetone solutions. After dehydration, the specimens were permeated with acetone containing embedding medium and finally cured in an oven at 37 °C. After embedding, the samples were further hardened in an oven at 60 °C for 48 h. The embedded samples were sectioned into ultrathin slices of 60–80 nm using an ultramicrotome, stained with uranyl acetate and lead citrate, and then observed and analyzed using a transmission electron microscope.

Analysis of EAEAR Components

Sample preparation: A total of 50 mg of the ethyl acetate extract of *Althaea rosea* flower freeze-dried powder was accurately weighed and then placed in a 1.5 mL EP centrifuge tube. Add precisely 1.00 mL methanol. Vortexing was conducted for 3 min, followed by ultrasonic extraction for 30 min. The extract was transferred to an ultrafiltration tube (molecular weight cut-off: 3×10^3 Da) and centrifuged at 14,000 rpm for 5 min. The supernatant was filtered through a 0.22 μm PTFE microporous membrane, the first filtrate was discarded, and the subsequent filtrate was retained for analysis.

Chromatographic conditions: The chromatographic column used was a Waters ACQUITY UPLC HSS T3 (3.0×100 mm, 1.8 μm). The mobile phase consisted of 0.1% formic acid in water (water phase: A) and acetonitrile (organic phase: B). The flow rate was 0.3 mL/min, the injection volume was 5 μL, and the column temperature was maintained at 40 °C. The gradient elution program was as follows: 0–2 min, 5% B; 2–42 min, 5–95% B; 42–47 min, 95% B; 47.1–50 min, 5% B.

Screening of active constituents with UPLC-Q-Orbitrap-HRMS: The analysis was performed using an electrospray ionization source (ESI) in positive and negative ion modes. The spray voltage was set to 3.2 kV for positive ions and 2.5 kV for negative ions. The capillary temperature was set at 320 °C, the sheath gas flow rate was 40 arb, and the auxiliary gas flow rate was 15 arb. A full scan/dd-MS2 approach was used for data acquisition. The resolution was set to 70,000 FWHM for the full scan and 17,500 FWHM for the MS2 scan. The full mass scan range was *m/z* 70–1,500, with an isolation window of 0.7 m/z. The normalized collision energies (NCE) were set to 15, 30, and 45 eV. Prior to injection, the mass axis of the mass spectrometer was calibrated using a calibration solution to ensure that the mass deviation was less than 5×10^{-6}. The discharge current was set to 4.0 μA, the ion transfer tube temperature was 350 °C, and the evaporation temperature was 350 °C, with an automatic gain control (AGC) target of 1×10^{6}.

Data processing: Raw mass spectrometry data were processed using Xcalibur™ 4.1 software for peak extraction and matching analysis. Screening and identification were conducted using TraceFinder 4.1 software, and the results were matched against the Traditional Chinese Medicine database. The main parameters set in TraceFinder 4.1 were as follows: mass error of m/z < 5×10^{-6}, intensity threshold > 5×10^{3}; product ions: at least one fragment ion present with an intensity threshold > 1,000 and a mass error of m/z < 5×10^{-6}; isotopic pattern: fit threshold > 80%, mass error < 5×10^{-6}, and intensity deviation < 20%.

Network Pharmacology Analysis

The CAS numbers of the 35 active components identified through UPLC-Q-Exactive-HRMS screening were input into the PubChem database (https://pubchem.ncbi.nlm.nih.gov/) to obtain the Canonical SMILES format for each component. The obtained files were then imported into the SwissADME platform (http://swissadme.ch/), and parameters were set to predict the potential targets of the active components of EAEAR.

Using "Tetrodotoxin" and "TTX" as keywords, target sites were identified through databases, such as GeneCards (https://www.genecards.org/) and OMIM (https://omim.org/). The results from multiple databases were merged, and duplicates were removed to finalize the target sites for TTX. Subsequently, Venny 2.1.0 (http://bioinfogpcnb.csices/tools/venny/) was used to perform intersection analysis between the target sites of EAEAR's active components and those of TTX, with the intersection targets considered potential targets for EAEAR intervention in TTX poisoning.

The intersected targets were then imported into the STRING database (https://string-db.org/) to construct a protein–protein interaction (PPI) network. The PPI network was saved as a.tsv file and imported into the Cytoscape 3.9.1 software. The key targets identified from the PPI network were further analyzed for gene ontology (GO) biological processes and Kyoto Encyclopedia of Genes and Genomes (KEGG) pathway enrichment using the DAVID 6.8 platform (https://david.ncifcrf.gov/). Through Cytoscape 3.9.1, the pathways were selected, and the relationships between EAEAR's active components, the intersected targets of TTX poisoning, and related signaling pathways and diseases were integrated into a "component–target–pathway" network. This analysis allowed for the identification of key targets and key pharmacodynamic components of EAEAR for intervention in TTX poisoning.

Metabolomics Analysis

Sample Preparation

For the metabolomics study, the control group, the TTX intoxication model group (Model), and the TTX+high dose EAEAR group (EAEAR) from "Animal modeling and dosing regimens" section were selected. Serum samples were prepared as follows: 100 μL of serum was precisely measured into an EP tube, and 400 μL of extraction solution (methanol: acetonitrile = 1:1, v/v) was added; the mixture was vortexed for 30s. The samples were then sonicated in an ice water bath for 10 min and allowed to stand at −40 °C for 1 h. The samples were then centrifuged at 12,000 rpm for 15 min at 4 °C. The supernatant was transferred to injection vials for analysis. An equal volume of 50 μL from each sample's supernatant was pooled to create quality control (QC) samples. The QC samples were run 10 times before analyzing the test samples and once every five test samples to evaluate the stability of the mass spectrometry system and data reproducibility.

UPLC-Q-Orbitrap HRMS Detection

Chromatographic conditions: Target compounds were separated on a Waters ACQUITY UPLC BEH Amide column (2.1 mm × 100 mm, 1.7 μm). The mobile phase A consisted of 25 mmol/L ammonium acetate and 25 mmol/L ammonia in water, and the mobile phase B was acetonitrile. The flow rate was set at 0.3 mL/min, the column temperature was 35 °C, the sample tray temperature was at 4 °C, and the injection volume was 2 μL. The gradient elution program was as follows: 0–0.5 min, 95% B; 0.5–7 min, 95–65% B; 7–8 min, 65–40% B; 8–9 min, 40% B; 9–9.1 min, 40–95% B; 9.1–12 min, 95% B.

The ion source was a HESI source, and the scanning mode was set to simultaneous positive and negative ion modes. The monitoring mode used was full scan/dd-MS^2, with a full scan resolution of 70,000 FWHM and a dd-MS2 resolution of 17,500 FWHM. The capillary temperature was 320 °C, the sheath gas flow rate was 40 arb, the auxiliary gas flow rate was 15 arb, the full scan mass range (*m*/*z*) was 70–1500, the isolation window (m/z) was 1.0, and the NCE was set to 15, 30, and 45 eV. Discharge current was 4.0 μA, ion transfer tube temperature was 350 °C, evaporation temperature was 350 °C, and AGC was 1×10^6.

Data Processing and Analysis

The raw data files were converted from.wiff to.mzXML format using ProteoWizard software and then imported into an R package for preprocessing, which included peak recognition, peak alignment, grouping, and annotation of isotopic ions, adduct ions, and fragment ions. The final output was a two-dimensional data matrix containing mass-to-charge ratio (m/z), retention time, and peak area information. Data points with missing values exceeding 50% in any group were filtered out, and missing values and zeros were filled using the "half of the minimum value" method.

The preprocessed two-dimensional data matrix was imported into SIMCA software (V16.0.2, Sartorius Stedim Data Analytics AB, Umea, Sweden) for multivariate statistical analysis. Subsequently, orthogonal partial least squares discriminant analysis (OPLS-DA) was conducted to identify differences between the control and model groups and between the TTX+EAEAR and TTX model groups and to screen for differential metabolites. Based on the high-resolution *m*/*z* values of the differential metabolites and in combination with secondary mass spectrometry data, potential structures of differential metabolites after EAEAR intervention were identified through online databases, such as HMDB (http://www.hmdb.ca/), LIPIDMAPS (https://www.lipidmaps.org/), GNPS (http://gnps.ucsd.edu/), and METLIN (https://metlin.scripps.edu/). The validated differential metabolites were exported and subjected to metabolic pathway enrichment analysis and topology analysis using the MetaboAnalyst 5.0 platform (http://www.metaboanalyst.ca) to identify relevant metabolic pathways following EAEAR intervention.

Integrated Network Pharmacology and Metabolomics Confluence Analysis

The 15 differential metabolites identified through metabolomics and the 15 key targets selected via network pharmacology were simultaneously imported into the MetaboAnalyst 5.0 platform (https://www.metaboanalyst.ca/). The Joint-pathway analysis module was utilized for integrated pathway analysis. Moreover, the key target proteins on the combined pathway were verified by Western blotting or ELISA, and UPLC-QqQ-MS/MS was applied to verify the differential metabolites of the intersecting metabolic pathways.

Western Blotting

The cerebral cortex samples were lysed in RIPA buffer supplemented with PMSF, followed by centrifugation to obtain the protein supernatant. Total protein concentration was determined by the BCA assay. Samples were boiled and then electrophoresed in a 10% separating gel, followed by membrane transfer. The membranes were blocked with 5% skimmed milk and then incubated overnight at 4 °C with primary antibodies (β-actin 1:2000, MAOA, AOC1, ALDH7A1, NAGS 1:1000). After washing with TBST, the membranes were incubated with secondary antibodies (1:5000) for 1.5 h at room temperature. Finally, the PVDF membranes were treated with a chemiluminescent substrate, exposed, and the protein bands were quantified using Image J software.

Enzyme-Linked Immunosorbent Assay

A total of 60 ± 0.5 mg of rat cerebral cortex samples were accurately weighed, and nine times the volume of homogenization medium (PBS: 50×Cocktail: phosphorylation inhibitor: PMSF = 100:2:1:1) was added at a ratio of weight (mg): volume (μL) = 1:9 and mechanically homogenized under the condition of ice water bath to form a 10% homogenate. Finally, the homogenate was centrifuged at 4 °C, 3000 rpm/min for 10 min, and the supernatant was collected to determine the levels of NOS1, NOS2, and NOS3 in the cerebral cortex according to the ELISA kit method.

UPLC-QqQ-MS/MS Analysis of Metabolites and Absorbed Constituents

The detection conditions were identical to those described in "Neuromodulatory small molecule analysis" section. The ion information, cone voltage, and collision energy parameters for the differential metabolites and core components of EAEAR in the blood are detailed in Supplementary Tables 1 and 2.

Statistical Analysis

The experimental data were analyzed using SPSS 23.0 software. First, normality and homogeneity of variance tests were performed. For data that followed a normal distribution with homogeneous variances, comparisons between multiple groups were performed using one-way ANOVA, while comparisons between two groups were conducted using an independent sample *t*-test. For data that did not meet the criteria for normality or homogeneity of variances, the Kruskal–Wallis *H*-test was used. Results are presented as mean ± standard deviation ($\bar{x} \pm s$, n = 10), with a significance level of $P < 0.05$.

Results

Effects of EAEAR in Alleviating TTX Poisoning in Rats

Protective Effect of EAEAR Against Cortical Damage in TTX-Intoxicated Rats

On the basis of the literature[13] and previous research by our group, the TTX-intoxicated model group was administered a single dose of 11.75 μg/kg TTX. The model group showed signs of lethargy, slow responses, reduced muscle tone, hind limb weakness with paw turned outward, dragging gait, reduced activity, and even abdominal breathing, although no mortality was observed. After intervention with different doses of EAEAR, the intoxication symptoms were alleviated in comparison with the model group.

Transmission electron microscopy was used to observe the effects of low, medium, and high doses of EAEAR on TTX-induced cortical pathological damage in rats. In the control group (Figure 1A), neuronal cell membranes were intact, organelles were structurally normal, the cytoplasm was homogeneous, and the nuclei were round with intact nuclear membranes, normal perinuclear space, and evenly distributed chromatin. In the TTX-intoxicated model group (Figure 1B) and the EAEAR-L intervention group (Figure 1C), severe neuronal cell damage was observed, including substantial shrinkage, cytoplasmic condensation with high electron density, aggregation, vacuolation, and irregular nuclear shape, though the nuclear membrane remained intact and heterochromatin increased. Pathological damage to the cerebral cortex of rats in the EAEAR-M group (Figure 1D) and EAEAR-H group (Figure 1E) was ameliorated and restored to the level of the control group. As shown in Figures 1D and E, TTX-intoxicated rats treated with high or medium doses of EAEAR showed intact cell membrane structure, normal organelle structure, homogeneous cytoplasm, rounded nuclei, intact nuclear membranes, normal perinuclear space, and evenly distributed chromatin in the cerebral cortex of rats. The results showed that high and medium doses of EAEAR considerably ameliorated neuronal damage and repaired neuronal cells in the cerebral cortex of TTX poisoned rats.

Effect of EAEAR on Four Neuromodulatory Small Molecules

Four neuromodulatory small molecules were determined in the serum of different groups of rats according to "Neuromodulatory small molecules analysis" (MRM spectra are shown in Figure 1J). Compared with the control group, the levels of L-proline (Pro) (Figure 1G) and L-acetylcarnitine (ALCAR) (Figure 1I) were significantly decreased in the model group ($P < 0.01$), whereas the levels of γ-aminobutyric acid (GABA) (Figure 1F) and N-acetyl-L-phenylalanine (N-Ac-L-Phe) (Figure 1H) were significantly increased ($P < 0.01$). After treatment with different doses

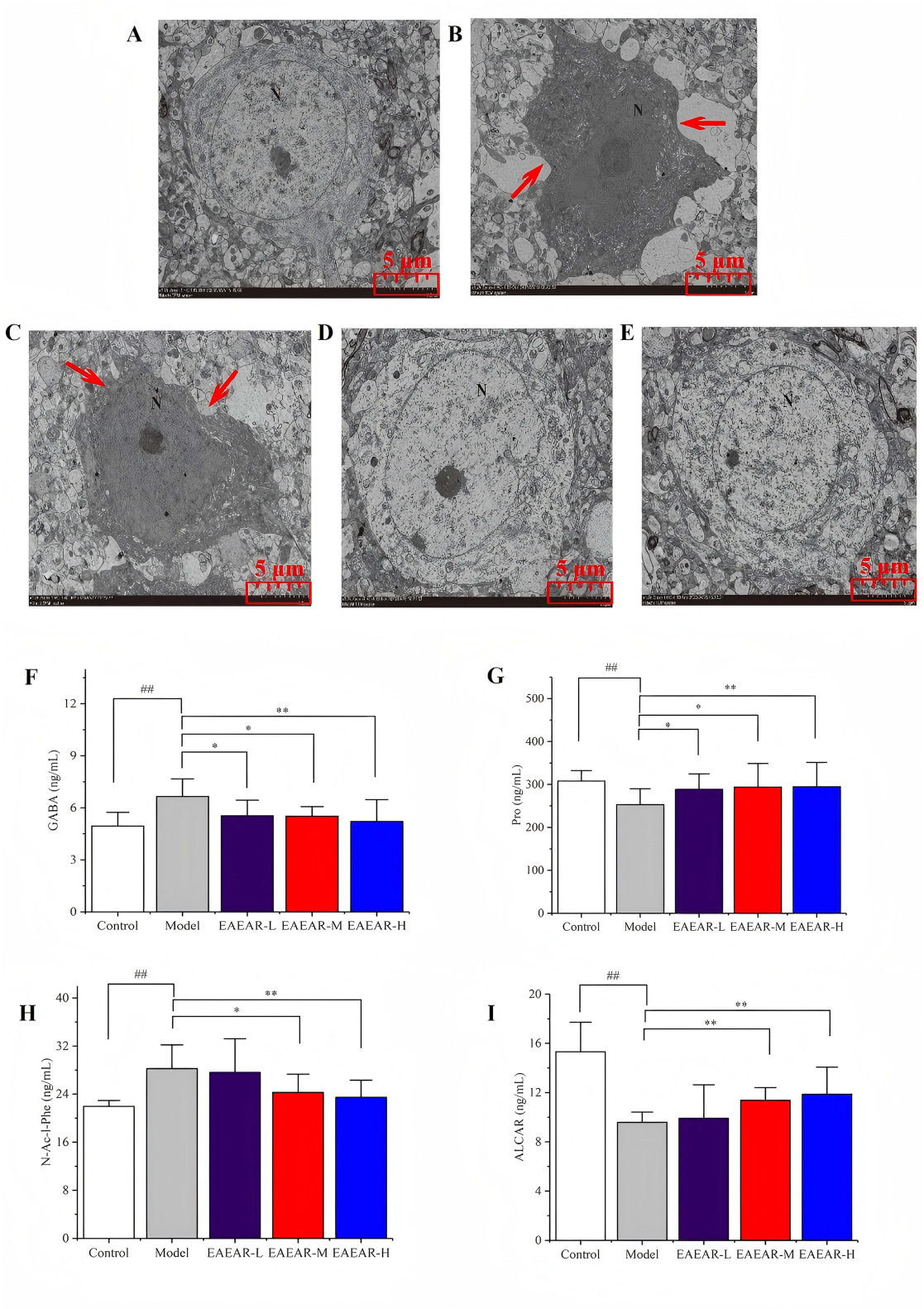

Figure 1 Continued.

https://doi.org/10.2147/DDDT.S505270

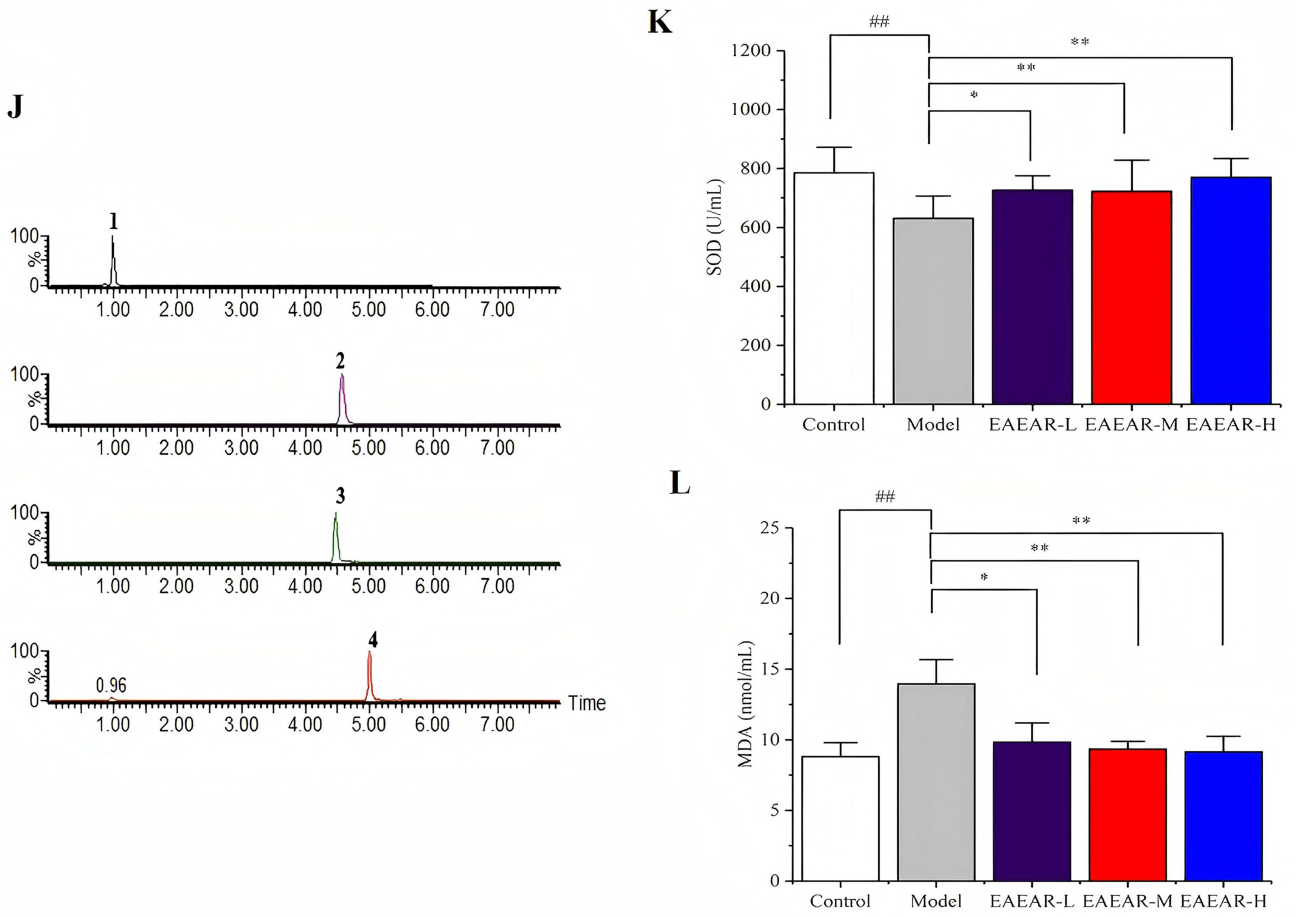

Figure 1 Effects of EAEAR in alleviating tetrodotoxin poisoning in rats. Ultrastructure of the cerebral cortex in **(A)** Control group and in **(B)** Model group (1,200×), respectively. Ultrastructure of the cerebral cortex in **(C)** EAEAR-L group and in **(D)** EAEAR-M group and in **(E)** EAEAR-H group (1,200×), respectively. **(F)** The levels of GABA in rat serum. **(G)** The levels of Pro in rat serum. **(H)** The levels of N-Ac-L-Phe in rat serum. **(I)**The levels of ALCAR in rat serum. **(J)** MRM chromatograms of four four neuromodulatory small molecules in rat serum (1. N-Ac-L-Phe, 2. ALCAR, 3. Pro, 4. GABA). **(K)**The levels of SOD in rat serum. **(L)**The levels of MDA in rat serum. Red arrows indicate the location of the lesion. ## indicates comparison between EAEAR group and model group with $P < 0.01$. * and ** refer to the comparison between EAEAR group and model group with $P < 0.05$ and $P < 0.01$, respectively.

of EAEAR, ALCAR levels were significantly increased in the EAEAR-M and EAEAR-H groups compared with the model group ($P < 0.01$), while N-Ac-L-Phe levels were significantly decreased ($P < 0.01$); however, no significant changes were observed in these neuromodulators in the EAEAR-L group ($P > 0.05$). The Pro levels were significantly increased ($P < 0.05$), and GABA levels were significantly decreased ($P < 0.05$) in all EAEAR-treated groups. Compared with the EAEAR-L group, the EAEAR-M and EAEAR-H treatments exhibited more pronounced regulatory effects on these neuromodulatory small molecules.

Effects of EAEAR on Oxidative Stress Indicators

The effect of EAEAR on the levels of SOD and MDA, biochemical indicators of oxidative stress in the serum of TTX-intoxicated rats, is shown in Figures 1K and L. Compared with the control group, the TTX-poisoned model group demonstrated significantly decreased ($P < 0.01$) serum SOD levels and significantly increased ($P < 0.05$) MDA levels. After treatment with different doses of EAEAR, the SOD levels were significantly increased ($P < 0.05$), and MDA levels were significantly decreased ($P < 0.05$) in the serum of rats in the EAEAR-L, EAEAR-M, and EAEAR-H groups compared with the model group. These results indicate that different doses of EAEAR can modulate the oxidative stress levels in TTX-poisoned rats.

Network Pharmacology Analysis

Identification of Components in the EAEAR

A total of 35 chemical components in EAEAR were identified by UPLC-Q-Orbitrap-HRMS according to the method described in "Analysis of EAEAR components" Section, as shown in Supplementary Table 3 and Supplementary Figure 2. Among these, 23 active components were detected in the ESI (+) mode, including adenosine, harmane, anisic acid, rutin, quercetin-7-O-β-D-glucopyranoside, cinnamic acid, astragalin, kaempferol, coumaric acid, ferulic acid, tiliroside, nicotiflorin, retrochalcone, periplogenin, 3,5,7-trihydroxychromone, quercetin, catechin hydrate, 5,7,4′-trihydroxy-8-methylflavanone, naringenin, kushenol F, schisanhenol, usnic acid, and brassinolide. In the ESI (-) mode, 12 active components were detected, including shogaol, glabrene, isoliquiritin, protocatechuic acid, coixol, caffeine acid, hematoxylin, scopoletin, dihydrokaempferol, luteolin, taxifolin, and apigenin.

Screening the Potential Targets of EAEAR to Mitigate TTX Toxicity

Oral absorption and drug-likeness predictions were performed using the SwissADME platform, which resulted in the exclusion of six components that did not meet the criteria. From the 35 ingredients identified by EAEAR, 29 active ingredients were screened, as detailed in Supplementary Table 4. These 29 active components were screened through the Swiss Target Prediction and SuperPred databases, yielding 2,097 potential targets. The corresponding Canonical SMILES and the number of targets for each active component are provided in Supplementary Table 5. After removing duplicates among the targets, 610 unique targets were associated with the 29 active components of EAEAR.

To identify the targets of TTX, databases such as NCBI, OMIM, GeneCards, and TTD were searched. After merging and removing duplicate targets, 411 TTX-related targets were identified. As shown in Figure 2A, a Venn diagram analysis was performed using the Venny 2.1.0 platform to compare the 610 targets of EAEAR's active components with the 411 TTX-related targets. This analysis identified 91 overlapping targets that are considered the potential targets of EAEAR for mitigating TTX toxicity.

Protein–Protein Interaction Analysis

The intersecting targets were uploaded to the STRING database to construct a protein–protein interaction (PPI) network, as shown in Figure 2B. The constructed PPI network consisted of 87 nodes and 445 edges. Each active component of EAEAR corresponded to multiple targets, and each target was associated with several active components. Through analysis, the average values for degree, closeness centrality, and betweenness centrality were determined to be 9, 0.43434, and 0.0054565, respectively. Targets exceeding these average values in all three metrics were identified as key targets for EAEAR's intervention in TTX toxicity, resulting in the identification of 38 key targets.

GO Function and KEGG Pathway Enrichment Analysis

GO enrichment analysis revealed 259 terms under biological processes (BP), primarily involving synaptic transmission, cellular processes, metabolic processes, and G-protein-coupled receptor signaling pathways. Under cellular components (CC), 60 terms were identified, mainly covering the cytoplasm, myelin sheath, synapse, neuronal parts, and G-protein-coupled receptors. Molecular functions (MF) included 63 terms, with receptor activator activity, adenylate cyclase regulator activity, and G-protein coupled receptor activity being predominant. Figure 2C shows the top 10 GO enrichment analysis results for BP, CC, and MF. KEGG pathway annotation analysis of the 38 key targets from the PPI network revealed their involvement in 98 pathways. The top 20 pathways with the lowest p-values were selected as the core pathways for EAEAR's intervention in TTX toxicity, and a bubble chart was drawn, as shown in Figure 2D. The primary metabolic pathways for EAEAR's intervention in TTX toxicity include neuroactive ligand–receptor interaction, dopaminergic synapses, the Rap1 signaling pathway, the estrogen signaling pathway, and the cAMP signaling pathway.

"Component–Target–Pathway" Network Analysis

Cytoscape 3.9.1 was used to construct an "component–target–pathway" network for EAEAR intervention in TTX intoxication (Supplementary Figure 3). This network consists of 85 nodes and 271 edges. A total of 12 active components of EAEAR were identified with above average betweenness, closeness, and degree values: hematoxylin, apigenin, dihydrokaempferol, retrochalcone, luteolin, kaempferol, naringenin, periplogenin, 5,7,4′-trihydroxy-8-

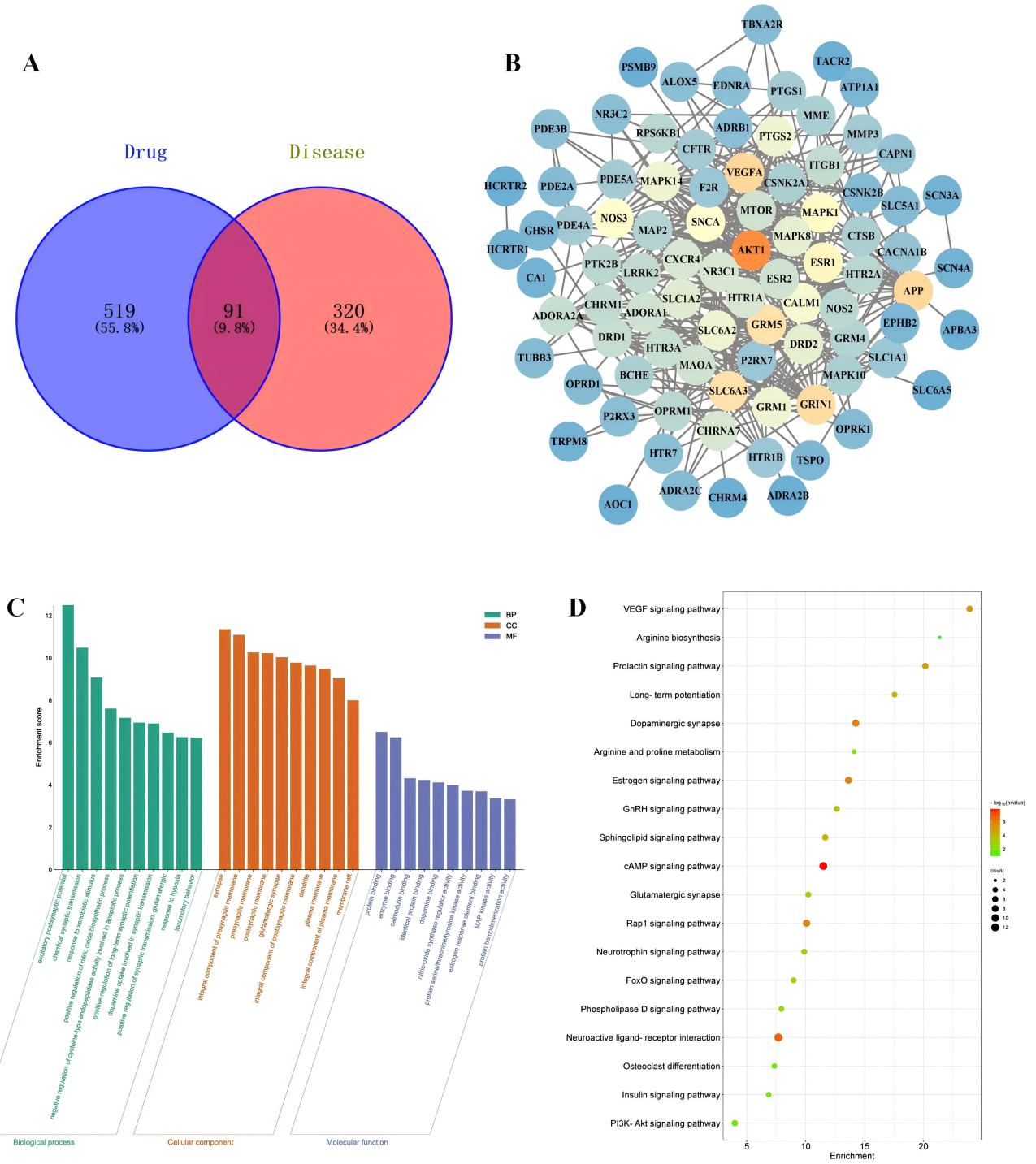

Figure 2 Network Pharmacology Analysis. **(A)** Venn diagram. **(B)** Protein–protein interaction network. **(C)** GO enrichment data, including GO molecular functions, GO cellular compositions, and GO biological processes. **(D)** KEGG pathway enrichment.

methylflavanone, glabrene, taxifolin, and caffeic acid (Table 1). Similarly, topological analysis was performed on key targets in "component–target–pathway" network, and 15 core targets whose betweenness, closeness, and degree are greater than the average were screened: ESR2, MAOA, ESR1, ADORA1, NOS2, PTGS2, GRM5, APP, ADORA2A, MAPK8, AKT1, CSNK2A1, ITGB1, CHRNA7, and NOS3 (Table 2).

Table 1 Active Components of EAEAR Identified by "Component–Target–Pathway" Network Analysis

No.	Components	Betweenness	Closeness	Degree
1	Hematoxylin	0.02886	0.43299	14
2	Apigenin	0.00809	0.40976	11
3	Dihydrokaempferol	0.01472	0.42640	11
4	Retrochalcone	0.01499	0.41379	11
5	Luteolin	0.00582	0.40580	10
6	Kaempferol	0.00582	0.40580	10
7	Naringenin	0.01208	0.41379	10
8	Periplogenin	0.01543	0.43299	10
9	5,7,4′-Trihydroxy-8-methylflavanone	0.00809	0.40976	9
10	Glabrene	0.01035	0.40191	9
11	Taxifolin	0.00562	0.40191	7
12	Caffeic acid	0.00467	0.39070	6

Table 2 Targets of EAEAR Identified by "Component–Target–Pathway"network Analysis

NO.	Targets	Betweenness	Closeness	Degree
1	ESR2	0.05234	0.52500	17
2	MAOA	0.04985	0.51852	16
3	ESR1	0.03346	0.50602	14
4	ADORA1	0.02977	0.50000	13
5	NOS2	0.02030	0.47458	13
6	PTGS2	0.02435	0.49412	12
7	GRM5	0.01524	0.47191	10
8	APP	0.01533	0.47727	9
9	ADORA2A	0.01608	0.47727	9
10	MAPK8	0.01477	0.47191	9
11	AKT1	0.01153	0.47191	8
12	CSNK2A1	0.00905	0.46667	7
13	ITGB1	0.00804	0.46154	7
14	CHRNA7	0.01132	0.46154	6
15	NOS3	0.01049	0.46154	6

https://doi.org/10.2147/DDDT.S505270

Metabolomics Study

On the basis of the UPLC-Q-Orbitrap-HRMS method for the identification of metabolites in each group of rat serum samples, the metabolites obtained from screening were subjected to unsupervised PCA analysis to examine the differences in metabolic patterns and the natural clustering trends among samples in each group. As shown in Figure 3, each data point in the figure represents the projection of a sample in a two-dimensional plane. The x-axis represents the contribution of the first principal component (PC1), while the y-axis represents the contribution of the second principal component (PC2). The PCA results indicate that in the ESI (+) and ESI (-) modes, the data points of the QC samples are closely clustered together, demonstrating minimal variability among the samples and confirming the stability and reliability of the instrument. The samples within each of the control, model, and EAEAR-intervention groups also show tight clustering, whereas the samples from different groups are clearly separated. This result suggests that significant changes in endogenous metabolites occurred in TTX-poisoned rats under the influence of EAEAR, leading to distinct metabolic profiles.

The OPLS-DA method was employed to analyze further the metabolic differences between the control and model groups, and between the EAEAR-treated and model groups. As shown in Figure 4, the score plots of the OPLS-DA models indicate a clear separation between the control and model groups (Figures 4A and B) and between the EAEAR-treated and model groups (Figures 4C and D) in the ESI (+) and ESI (-) modes. This separation indicates significant metabolic differences between the groups. A permutation test was performed to ensure the validity of the models and to avoid overfitting. The results of the permutation test, as shown in Figures 4E–H, reveal that the R^2Y values for each group are greater than 0.5, and the intercepts of Q^2 on the vertical axis are negative, indicating that no overfitting in the models.

On the basis of the OPLS-DA analysis model of the control and model groups, metabolites with a VIP > 1 were initially selected. These selected metabolites were then subjected to a *t*-test, and those with a $P < 0.05$ were identified as candidate differential metabolites. A total of 152 differential metabolites were identified in the serum of rats when comparing the control and model groups. Similarly, 347 differential metabolites were identified when comparing the EAEAR-treated and model groups. A Wayne diagram intersection analysis of the differential metabolites in the serum of rats screened in the control group versus the model group and the EAEAR group versus the model group yielded 31 differential metabolites (Supplementary Figure 4). A total of 15 differential metabolites that showed a reversal trend after

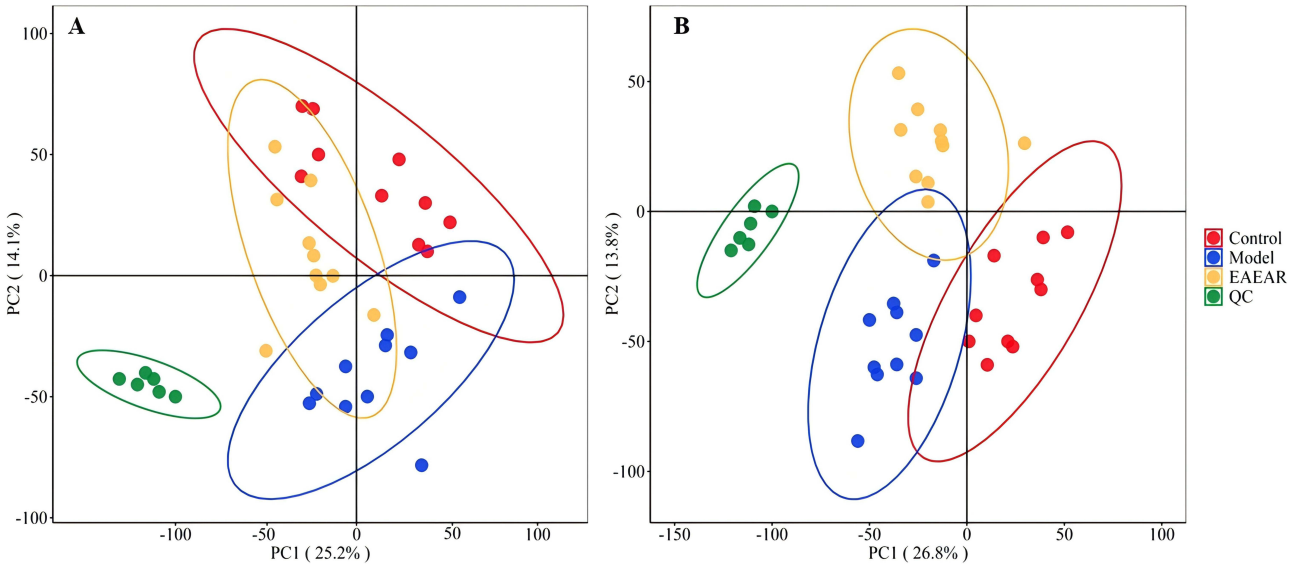

Figure 3 Score plots of PCA for different groupsESI(+) mode **(A)** and ESI(-) mode **(B)**. The colors red, blue, Orange, and green represent the control group, model group, EAEAR-treated group, and QC samples, respectively.

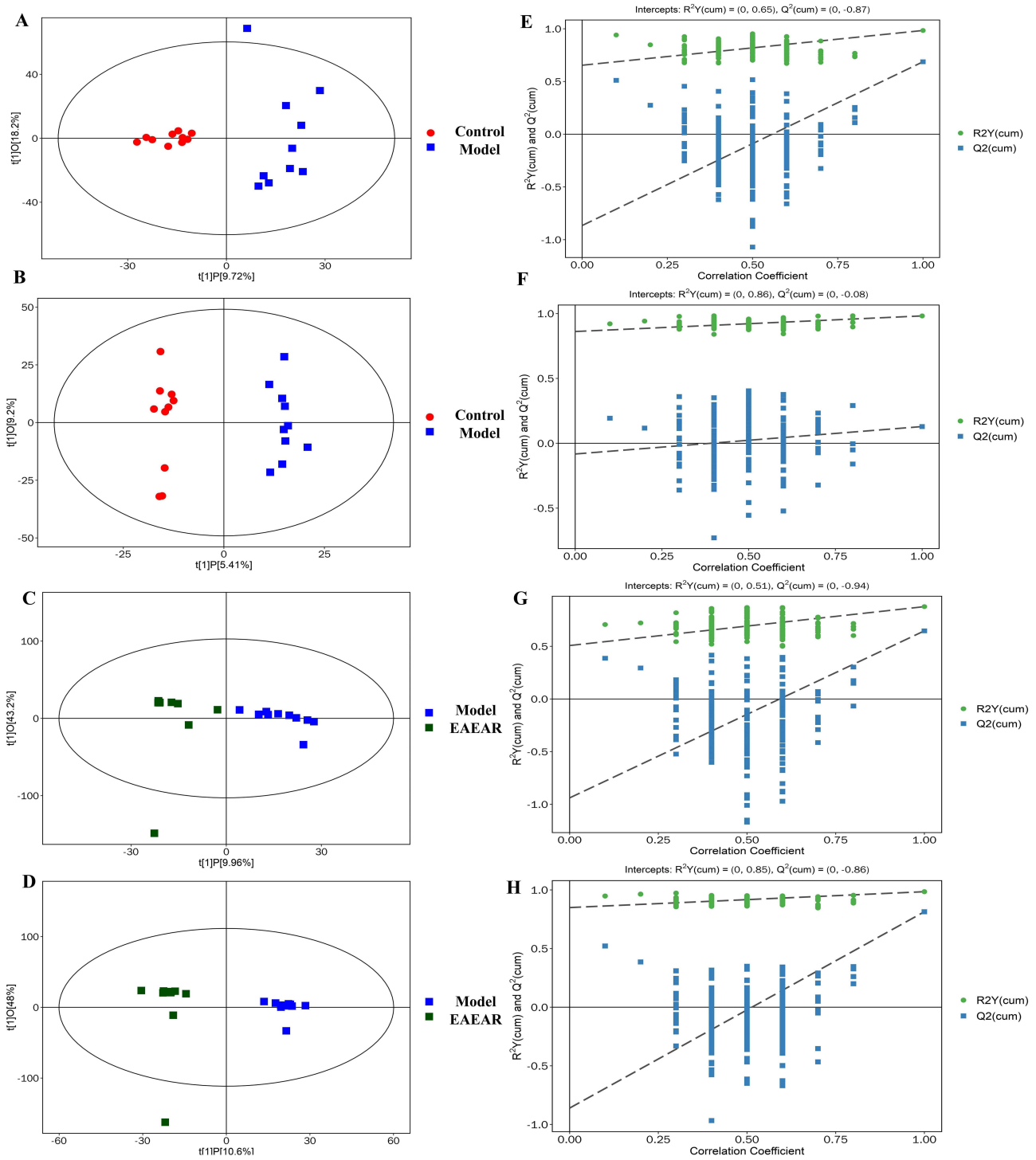

Figure 4 OPLS-DA score plots and permutation validation plots between the control group and the model group, and between the EAEAR group and the model group. OPLS-DA score plots of the control and model groups under ESI (+) mode **(A)** and ESI (-) mode **(B)**, respectively; Permutation validation plots of the control group and model group under ESI (+) mode **(E)** and ESI (-) mode **(F)**, respectively; OPLS-DA score plot of the EAEAR group and model group under ESI (+) mode **(C)** and ESI (-) mode **(D)**, respectively; Permutation validation plot of the EAEAR group and model group under ESI (+) mode **(G)** and ESI (-) mode **(H)**, respectively.

intervention in the EAEAR group were further investigated. The 15 differential metabolites were identified as ectoine, acetylhydrazine, N-ethylglycine, L-acetyl-carnitine, L-glutamate, 3-phospho-D-glyceroyl phosphate, diethanolamine, NADP+, NADPH, CDP-choline, 4-aminobutyric acid, L-proline, N-acetyl-L-glutamic acid, N-acetyl-L-phenylalanine, and pyruvic acid (Table 3).

https://doi.org/10.2147/DDDT.S505270

Table 3 Information Related to Differential Metabolites

NO.	Metabolites	RT (min)	MW(Da)	Ion mode	Formula	KEGG	Model vs Control	EAEAR vs Model
1	Ectoine	2.92	142.07423	$[M+H]^+$	$C_6H_{10}N_2O_2$	C07447	$\downarrow^{\#}$	$\uparrow^{*}$
2	Acetylhydrazine	5.65	74.04801	$[M+H]^+$	$C_2H_6N_2$	C06231	$\uparrow^{\#}$	$\downarrow^{*}$
3	N-Ethylglycine	5.55	103.06333	$[M+H]^+$	C_4H_9NO	C11735	$\uparrow^{\#}$	$\downarrow^{*}$
4	L-Acetyl carnitine	5.40	203.11575	$[M+H]^+$	$C_9H_{17}NO_4$	C02571	$\downarrow^{\#}$	$\uparrow^{*}$
5	L-Glutamate	4.83	145.03860	$[M+H]^+$	$C_5H_7NO_4$	C00025	$\downarrow^{\#}$	$\uparrow^{*}$
6	3-Phospho-D-glyceroyl phosphate	5.32	265.95926	$[M+H]^+$	$C_3H_8O_{10}P_2$	C00236	$\uparrow^{\#\#}$	$\downarrow^{**}$
7	Diethanolamine	4.96	105.07898	$[M+H]^+$	$C_4H_{11}NO_2$	C06772	$\downarrow^{\#}$	$\uparrow^{*}$
8	NADP+	3.75	744.08270	$[M+H]^+$	$C_{21}H_{29}N_7O_{17}P_3$	C00006	$\downarrow^{\#\#}$	$\uparrow^{**}$
9	NADPH	5.13	745.09112	$[M+H]^+$	$C_{21}H_{30}N_7O_{17}P_3$	C00005	$\downarrow^{\#\#}$	$\uparrow^{*}$
10	CDP-choline	0.55	488.10733	$[M-H]^-$	$C_{14}H_{26}N_4O_{11}P_2$	C00307	$\downarrow^{\#}$	$\uparrow^{*}$
11	4-Aminobutyric acid	5.72	103.06333	$[M-H]^-$	$C_4H_9NO_2$	C00334	$\uparrow^{\#}$	$\downarrow^{**}$
12	L-Proline	1.13	115.06333	$[M-H]^-$	$C_5H_9NO_2$	C00148	$\downarrow^{\#}$	$\uparrow^{**}$
13	N-Acetyl-L-glutamic acid	6.65	189.06372	$[M-H]^-$	$C_7H_{11}NO_5$	C00624	$\uparrow^{\#}$	$\downarrow^{**}$
14	N-Acetyl-L-phenylalanine	3.25	207.08954	$[M-H]^-$	$C_{11}H_{13}NO_3$	C03519	$\uparrow^{\#}$	$\downarrow^{*}$
15	Pyruvic acid	3.86	88.01604	$[M-H]^-$	$C_3H_4O_3$	C00022	$\uparrow^{\#\#}$	$\downarrow^{*}$

Note: $^{\#}$ indicates $P < 0.05$ compared to the Control group; $^{\#\#}$ indicates $P < 0.01$ compared to the Control group. * indicates $P < 0.05$ compared to the Model group; ** indicates $P < 0.01$ compared to the Model group. "↓" or "↑" indicates increased or decreased levels of the metabolites, respectively.

Integrative Analysis of Network Pharmacology and Metabolomics

Identification of Pathways and Key Targets

The 15 differential metabolites screened by above metabolomics and the 15 key targets screened by network pharmacology in the "component–target–pathway network analysis" Section were simultaneously imported in the MetaboAnalyst 5.0 platform, and joint pathway analysis was conducted by using the Joint-pathway Analysis-Module. The analysis module was used with the following parameter settings: targets Organism select Homo sapiens (human), and differential metabolite Metabolomics Type select Targeted (compound list). The results are shown in Supplementary Table 6. A total of 21 pathways were mapped in the combined pathway analysis, of which the top two in terms of impact and $-\log_{10}(p)$ values were arginine and proline metabolism and arginine biosynthesis. The impact values of these two pathways were 0.28 and 0.38, both greater than 0.1, with −log10(p) of 7.1267 and 4.9565, respectively.

The joint pathway analysis bubble diagram is shown in Figure 5. Each bubble in the graph represents a metabolic pathway, and the horizontal coordinate and bubble size indicate the size of the influence factor of the pathway in the topological analysis, and the larger the bubble, the larger the influence factor; the vertical coordinate and the bubble color indicate the p-value of the enrichment analysis, and the more the color, the smaller the p-value and the more significant the degree of enrichment. The results showed that among the 21 pathways, two pathways, arginine and proline metabolism pathway and arginine biosynthesis metabolism pathway, had the darkest color and the most significant enrichment degree. The four differential metabolites (L-glutamate, GABA, Pro, and pyruvic acid) screened by metabolomics and the three key targets of network pharmacology (MAOA, NOS2, and NOS3) cointersected in the arginine and proline metabolic pathways. The two differential metabolites screened by metabolomics (GABA and L-Glutamate) and the two key targets of network pharmacology (NOS2, NOS3) collectively intersect in the arginine biosynthetic metabolic pathway.

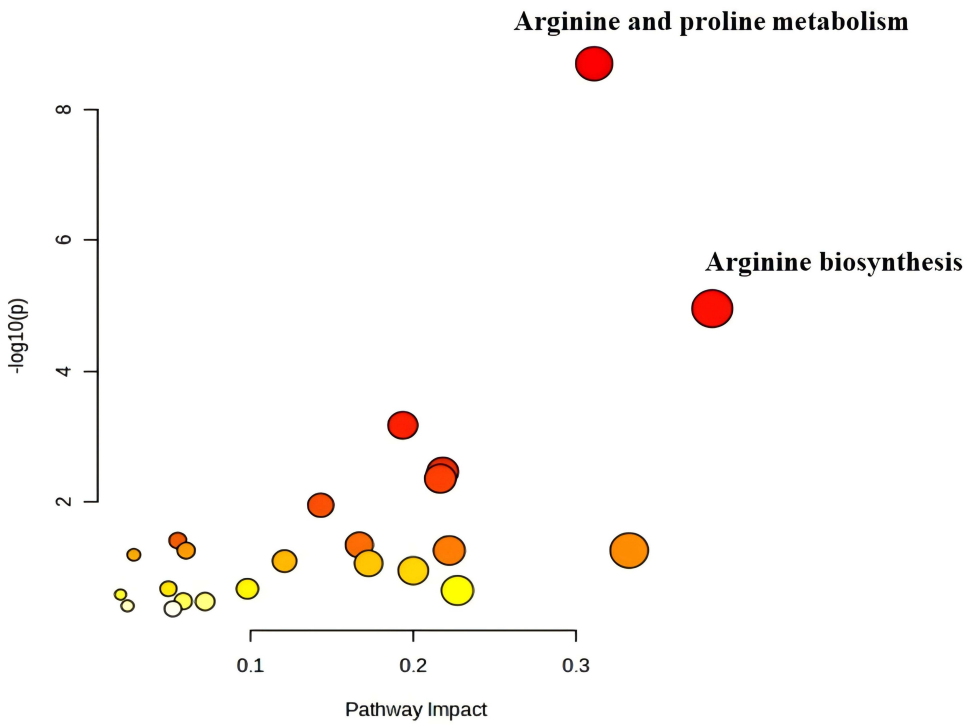

Figure 5 Joint-pathway Analysis of differential metabolites and key targets.

Validation of Key Targets by Western Blot and ELISA

The validation of key targets involved in the arginine and proline metabolism pathways, including MAOA, AOC1, ALDH7A1, NOS1, NOS2, and NOS3, as well as NAGS in the arginine biosynthesis pathway, was performed using Western blotting and ELISA. Additionally, the levels of the differential metabolites Pro, GABA, and NAG associated with these pathways were quantified using UPLC-QqQ-MS/MS.

Western blotting results are depicted in Figures 6A–E. Compared with the control group, the expression level of MAOA protein in the brain cortex of model rats was significantly decreased ($P < 0.01$), while the expression levels of AOC1, ALDH7A1, and NAGS proteins were significantly increased ($P < 0.05$). After EAEAR intervention in TTX-poisoned rats, the MAOA protein expression level in the cerebral cortex was significantly increased ($P < 0.01$) compared with the model group, whereas the expression levels of AOC1, ALDH7A1, and NAGS were significantly decreased ($P < 0.05$), that is, these protein expressions showed reverse adjustment.

ELISA assays were used to assess the effect of EAEAR on the NOS1, NOS2, and NOS3 proteins in the cerebral cortex of TTX-poisoned rats. As shown in Figures 6F and G, the expression levels of NOS1 and NOS2 proteins in the rat brain cortex of the TTX-poisoned model group were significantly reduced in the brain cortex of the TTX-poisoned model group compared with the control group ($P < 0.01$). After EAEAR treatment, the expression levels of NOS1 and NOS2 proteins in the brain cortex of the treated rats were significantly increased ($P < 0.05$) compared with the model group. However, the level of NOS3 was below the detection limit of the assay (0.1065 ng/mL) and could not be measured.

Validation of Differential Metabolites by UPLC-QqQ-MS/MS

The metabolites Pro and GABA associated with the arginine and proline metabolic pathways and the differential metabolite NAG in the arginine biosynthesis metabolic pathway were determined by UPLC-QqQ-MS/MS, and the MRM spectra are shown in Figure 7A. The results shown in Figures 7B–D indicate that the rat serum levels of Pro significantly decreased ($P < 0.01$) in the model group compared with the control group, whereas the levels of GABA and NAG were significantly increased ($P < 0.01$) after TTX intoxication. After EAEAR intervention, the serum levels of Pro in the treated rats were significantly increased ($P < 0.01$) in comparison with the model group, while the levels of GABA ($P < 0.05$) and NAG ($P < 0.01$) were significantly decreased, demonstrating a reversal in the levels of these three

https://doi.org/10.2147/DDDT.S505270

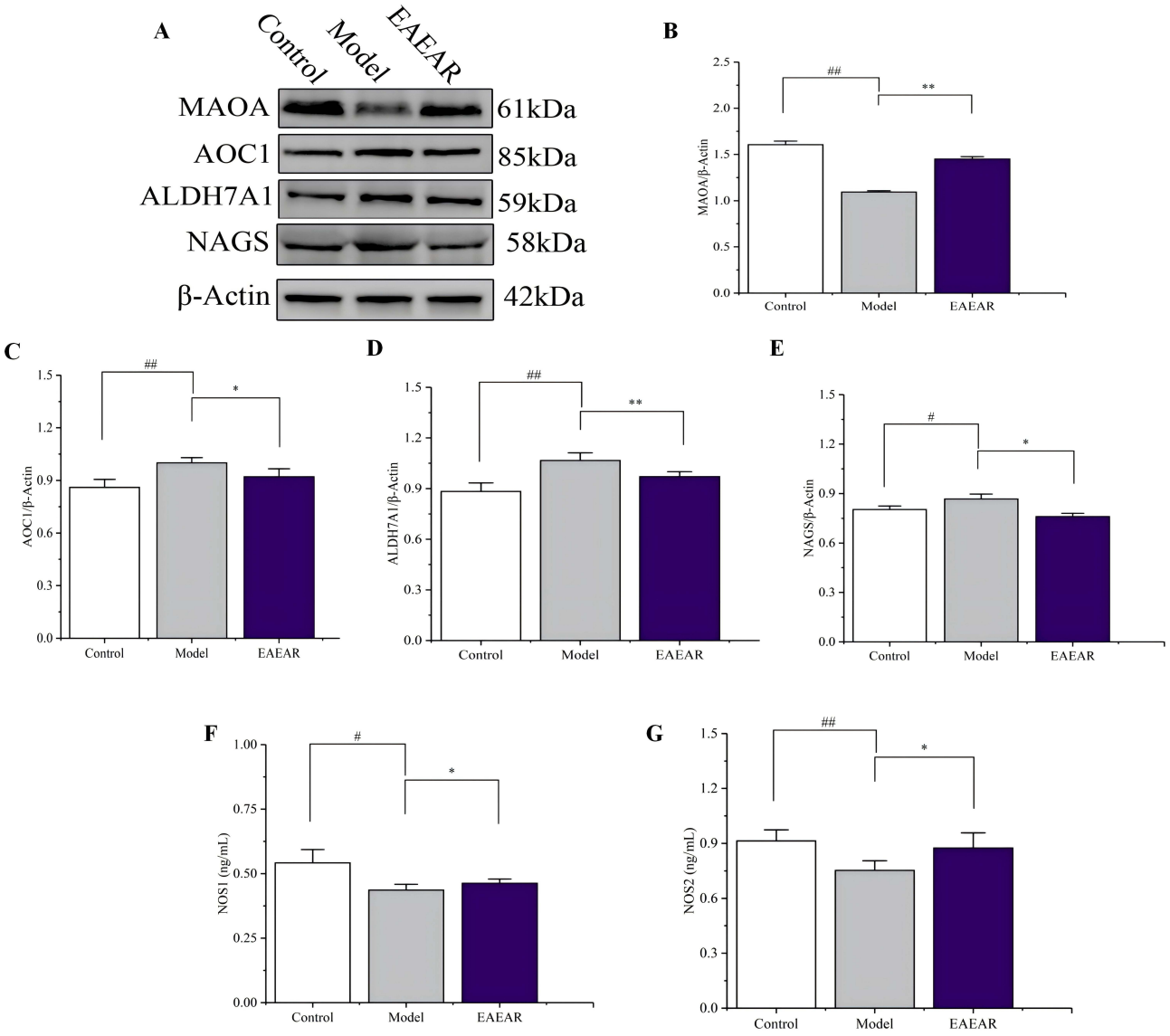

Figure 6 Experimental validation was performed on key targets. **(A)** Western blotting bands of relevant proteins in rat cerebral cortex. Quantification of the protein expression of **(B)** MAOA, **(C)**AOC1, **(D)**ALDH7A1, and **(E)** NAGS in rat cerebral cortex (n = 3). ELISA for determination of **(F)** NOS1 and **(G)** NOS2 in rat cerebral cortex (n = 5). The values are the means ± SD. # and ## refer to the comparison between EAEAR group and model group with $P < 0.05$ and $P < 0.01$, respectively. * and ** refer to the comparison between EAEAR group and model group with $P < 0.05$ and $P < 0.01$, respectively.

metabolites. The trends of the three differential metabolites validated by the UPLC-QqQ-MS/MS method were consistent with the results of the metabolomics study.

Determination of Core Components of Incoming Blood

A total of 11 active ingredients were successfully detected in the plasma of rats after EAEAR gavage using the method described in "UPLC-QqQ-MS/MS analysis of metabolites and absorbed constituents". These constituents include ferulic acid, naringenin, astragalin, quercetin-7-O-β-D-glucopyranoside, tiliroside, caffeic acid, scopoletin, apigenin, luteolin, dihydrokaempferol, and taxifolin. The MRM chromatograms of these absorbed components in rat plasma are shown in Supplementary Figure 5. Among the 12 core components identified by network pharmacology, five active constituents were detected in the rat plasma, including apigenin, luteolin, dihydrokaempferol, taxifolin, and naringenin.

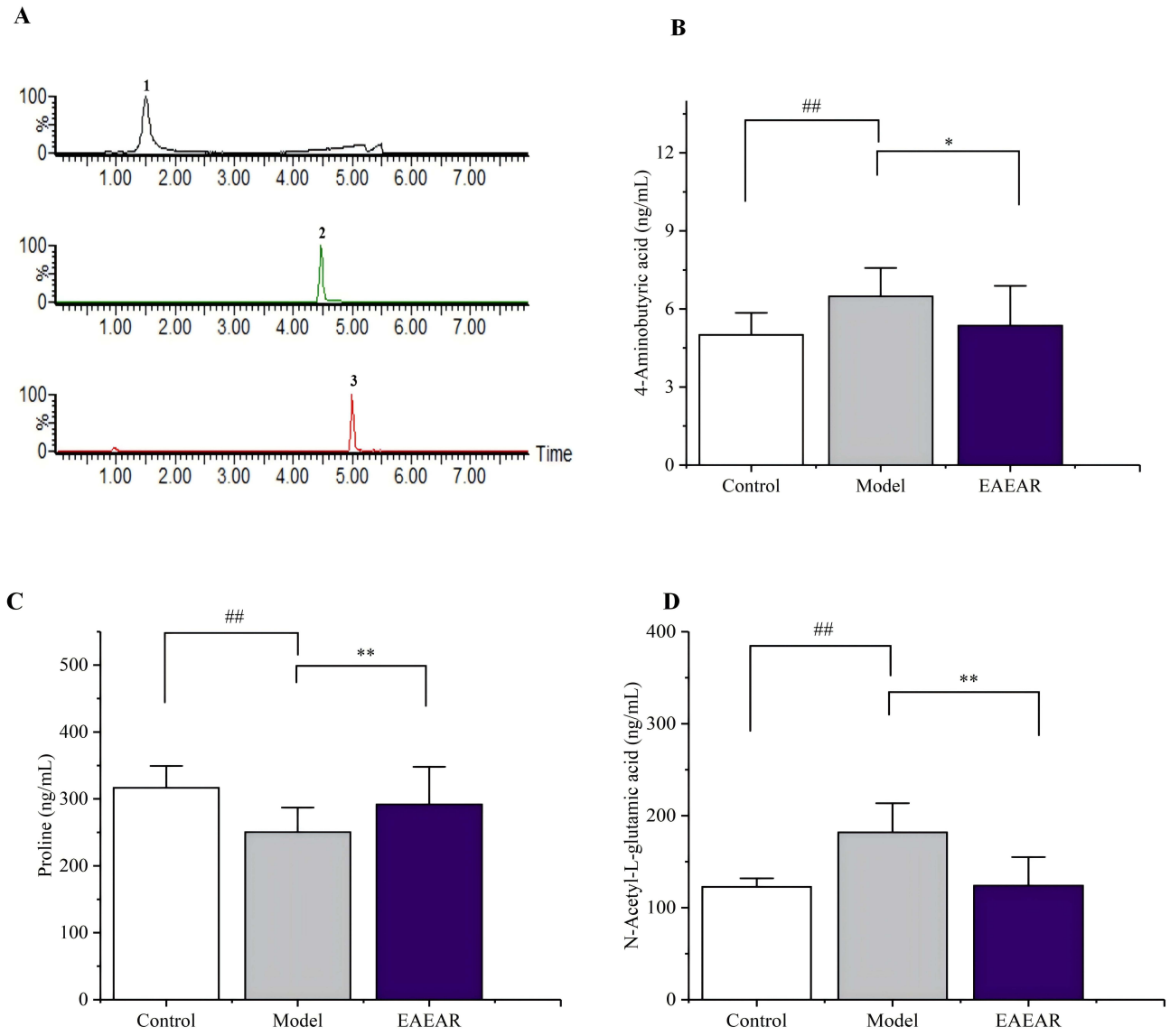

Figure 7 Validation of differential metabolites in TTX-intoxicated rats treated with EAEAR. **(A)** MRM plots of differential metabolites (1. NAG, 2.Pro, 3.GABA), **(B)** GABA, **(C)** Pro, **(D)** NAG. The values are the means ± SD (n = 5). ## refer to the comparison between EAEAR group and model group with $P < 0.01$. * and ** refer to the comparison between EAEAR group and model group with $P < 0.05$ and $P < 0.01$, respectively.

Discussion

Combined metabolomics and network pharmacology analyses of the 15 differential metabolites screened and the 15 key targets predicted in network pharmacology led to the identification of two key pathways for the administration of EAEAR to intervene in TTX intoxication: the arginine and proline metabolism pathway and the arginine biosynthesis pathway. As a comprehensive metabolic pathway, arginine and proline metabolism involves the interconversion and regulation of arginine and proline, which plays various important physiological functions in animals, including protein and energy metabolism and immune regulation.[14] The arginine biosynthetic pathway is involved in NO biosynthesis, regulation of cell proliferation and differentiation, and immune responses in organisms[15] and involves key enzymes such as ornithine aminotransferase, ornithine amidohydrolase, and arginine synthase.[16]

This study experimentally validated six targets within the arginine and proline metabolism pathway (ie, MAOA, AOC1, ALDH7A1, NOS1, NOS2, and NOS3) and two differential metabolites (ie, Pro and GABA). The results indicated a significant reversal of these indicators in the EAEAR intervention group compared with the model group. MAOA, a monoamine oxidase, plays a crucial role in the nervous system by primarily degrading and metabolizing

https://doi.org/10.2147/DDDT.S505270

monoamine compounds in neurotransmitters.[17] MAOA can regulate the activity of certain neurotransmitter receptors, indirectly modulate second messenger systems (such as cAMP), and influence sodium channel activity, thereby participating in the detoxification processes associated with TTX-induced poisoning.[18,19] AOC1, an amine oxidase, regulates neurotransmitter release and neuronal excitability and is involved in the synthesis of GABA. Elevated AOC1 levels can lead to the accumulation of GABA.[20] ALDH7A1, an aldehyde dehydrogenase, is involved in the degradation of proline and the metabolism of arginine. It converts proline into glutamate and arginine into nitric oxide (NO) and urea. The activity of AOC1 affects arginine metabolism, thereby affecting proline production, which is a primary function of ALDH7A1. Consequently, AOC1 activity indirectly regulates ALDH7A1 function.[21] Studies have shown that ALDH7A1, like AOC1, can affect GABA metabolism and energy production pathways.[22] As the primary inhibitory neurotransmitter in the brain, increased GABA levels can lead to reduced blood pressure, drowsiness, and fatigue. Previous research found that GABA levels increased in rats after TTX intoxication and gradually returned to normal after EAEAR intervention.[13] The validation results of this study revealed that EAEAR was able to reduce the protein expression of AOC1 and ALDH7A1, thereby inhibiting their activities, reducing the accumulation of GABA, alleviating the symptoms of intoxication, and possibly playing a role in the treatment of TTX intoxication.

Nitric oxide synthase (NOS) is a vital bioactive molecule responsible for converting L-arginine into NO. NOS includes three different isoforms: NOS1, NOS2, NOS3, all of which catalyze the metabolism of L-arginine to NO.[23] NO functions as a unique neurotransmitter, modulating sensory nerve transmission, dilating blood vessels, and participating in inflammatory responses.[24] Additionally, NO production may increase the activity or permeability of sodium ion channels, thereby affecting nerve conduction and intracellular ion balance.[25] In particular, NO can influence voltage-gated sodium channels (VGSCs), which are critical for the initiation and propagation of action potentials in neurons.[26] By modulating the opening and closing of VGSCs, NO may alter the excitability of nerve cells, thereby affecting signal transmission and contributing to the overall neurophysiological response to TTX poisoning.The results of significant reversal of NOS1 and NOS2 in the EAEAR intervention group compared with the model group suggest that EAEAR may play its role in interfering with TTX intoxication by regulating NO through increasing the expression of NOS1 and NOS2 proteins.

The experimental validation of the key protein NAGS and the metabolite NAG in the arginine biosynthesis pathway showed a significant reversal in the EAEAR intervention group compared with the model group. NAGS is a glutamate assimilating enzyme, and its activity directly influences the rate of arginine synthesis.[27] Arginine serves as a precursor for NO production and plays a critical role in signal transduction and regulation in various physiological processes.[25,28] NAG is a metabolite produced by the NAGS-catalyzed reaction between glutamate and acetyl-CoA.[29] EAEAR may alleviate TTX toxicity by modulating NAGS and NAG, thereby affecting NO levels within the arginine biosynthetic pathway. By managing NAGS and NAG, EAEAR can change NO levels in the pathway for making arginine. This in turn alters the functioning of the VGSC. The modulation of NO production may help to stabilise VGSC activity and restore normal neuronal excitability, ultimately reducing the neurological damage caused by TTX poisoning.

Th key targets and metabolites with significant changes were mapped onto the KEGG metabolic pathways, with the primary mechanisms by which EAEAR alleviates TTX toxicity depicted in Figure 8, Supplementary Figure 6A and B. This study further experimentally validated that EAEAR exerts its therapeutic effects on TTX-intoxicated rats through two main mechanisms. The first is by modulating key proteins (NOS1, NOS2, MAOA, AOC1, and ALDH7A1) and the differential metabolites (GABA and Pro) in the arginine and proline metabolism pathway. This pathway, as an integrative metabolic route, involves the interconversion and regulation of arginine and proline and plays several crucial physiological roles in animals, including participation in protein and energy metabolism and immune regulation. Second, EAEAR modulates key proteins (NOS1, NOS2, NAGS) and the differential metabolite (NAG) in the arginine biosynthetic pathway. TTX intoxication causes brain damage in rats, leading to altered arginine metabolism. EAEAR enhances the activity of the arginine biosynthesis pathway, fulfilling the demand for arginine by NOS, thereby achieving its therapeutic effect.

The medicinal value of the *Althaea rosea* flower is closely related to its chemical constituents.[30] Of the 12 key components screened in the study via network pharmacology, five active compounds were detected in rat plasma: apigenin, luteolin, dihydrokaempferol, taxifolin, and naringenin. Literature reports indicate that apigenin,[31] naringenin,[32]

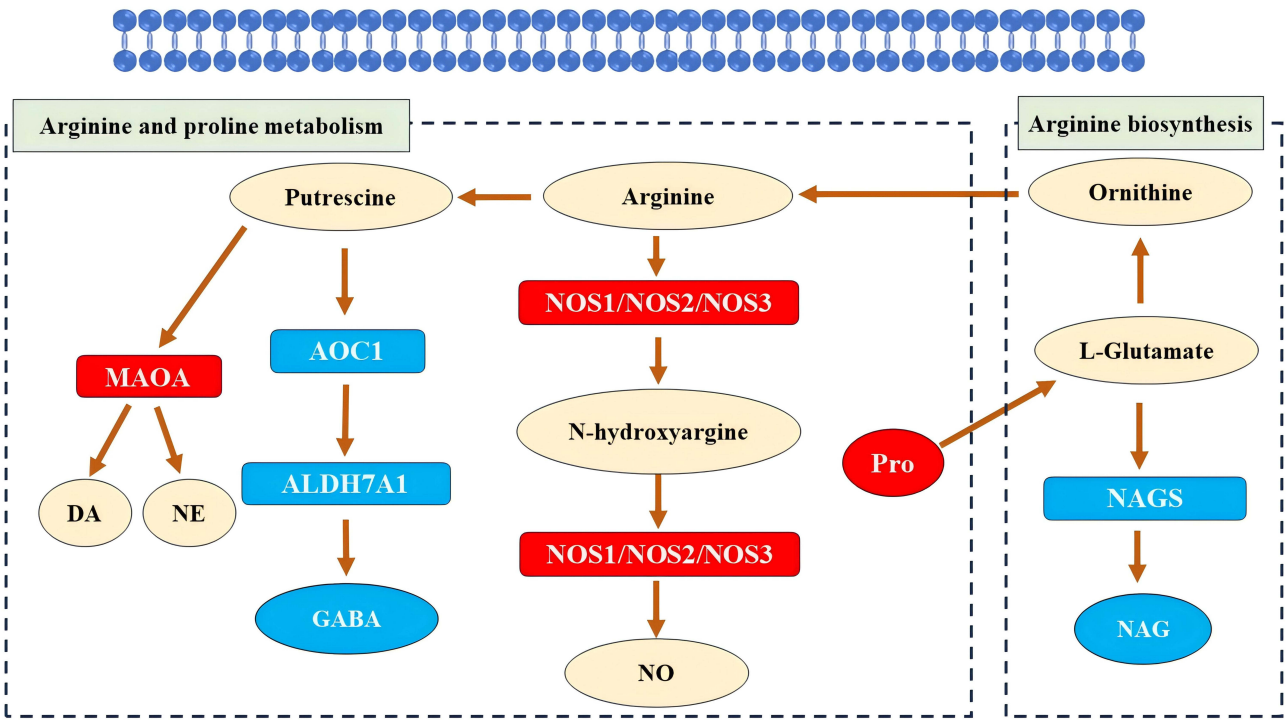

Figure 8 Diagram of the main mechanism of action of EAEAR in the treatment of TTX poisoning (red fill indicates up-regulation, blue fill indicates down-regulation).

and luteolin[33] possess antioxidant and anti-inflammatory properties that may help mitigate cellular damage caused by oxidative stress. Apigenin, a core component of EAEAR, exhibits a wide range of biological activities, including anti-inflammatory, antibacterial, antiviral, and anticancer effects.[34] Its primary action targets include ESR2, MAOA, ESR1, ADORA1, APP, ADORA2A, AKT1, and CSNK2A1, suggesting that apigenin may alleviate TTX toxicity through these key targets. Another key component, naringenin, is one of the herb's most important active ingredients, used primarily in organisms to reduce inflammatory responses by inhibiting the production and release of inflammatory mediators, such as prostaglandins and interleukins. Additionally, naringenin has potent antioxidant properties that can effectively scavenge free radicals in the body and protect cells from oxidative damage.[35] The key targets of naringenin include ESR2, MAOA, ADORA1, GRM5, NOS2, and ITGB1, suggesting that naringenin may exert its protective effects against TTX toxicity through these mechanisms.

Conclusion

This study integrates metabolomics and network pharmacology analyses to identify two key pathways through which EAEAR intervenes in TTX poisoning: the arginine and proline metabolism pathway and the arginine biosynthesis pathway. By using UPLC-QqQ-MS/MS, three differential metabolites (GABA, Pro, and NAG) within these overlapping pathways were detected, and six core target proteins (NOS1, NOS2, MAOA, AOC1, ALDH7A1, and NAGS) were successfully validated using Western blotting and ELISA techniques. The results suggest that EAEAR exerts its protective effect against TTX poisoning in rats by modulating the arginine and proline metabolism and arginine biosynthetic pathways. In addition, UPLC-QqQ-MS/MS analysis detected five absorbed constituents, ie, apigenin, luteolin, dihydrokaempferol, taxifolin, and naringenin, which overlap with the core constituents identified by network pharmacology. The integration analysis by metabolomics and network pharmacology helps to explore deeply the mechanisms of action of EAEAR in alleviating TTX toxicity in rats, which is crucial for the prevention and treatment of TTX poisoning.

https://doi.org/10.2147/DDDT.S505270

Abbreviations

ADORA1, adenosine a1 receptor; ADORA2A, adenosine a2a receptor; AKT1, serine/threonine kinase 1; ALCAR, L-acetylcarnitine; ALDH7A1, aldehyde dehydrogenase 7 family member a1; ANOVA, analysis of variance; AOC1, amine oxidase copper containing 1; APP, amyloid beta precursor protein; BP, biological process; CASP3, caspase 3; CC, cellular component; CE, collision energy; CHRNA7, cholinergic receptor nicotinic alpha 7 subunit; CSNK2A1, casein kinase 2 alpha 1; CV, cone voltage; EAEAR, ethyl acetate extract of *Althaea rosea* (Linn.) Cavan. flower; ELISA, enzyme linked immunosorbent assay; ESI, electrospray ionization; ESR1, estrogen receptor 1; ESR2, estrogen receptor 2; GABA, 4-aminobutyric acid; GO, gene ontology; GPCRs, g-protein coupled receptor; GRM5, glutamate metabotropic receptor 5; ITGB1, integrin subunit beta 1; KEGG, kyoto encyclopedia of genes and genomes; MAOA, monoamine oxidase a; MAPK1, mitogen-activated protein kinase 1; MAPK8, mitogen-activated protein kinase 8; MAPK14, mitogen-activated protein kinase 14; MCC, maximal clique centrality; MDA, malonic dialdehyde; MF, molecular function; MRM, multiple reaction monitoring; N-Ac-L-Phe, n-acetyl-L-phenylalanine; NAGS, n-acetylglutamate synthase; ND, not detected; NOS1, nitric oxide synthase 1; NOS2, nitric oxide synthase 2; NOS3, nitric oxide synthase 3; OPLS-DA, orthogonal projections to latent structures squares-discrimination analysis; PC1, principal component 1; PC2, principal component 2; PCA, principal component analysis; PPI, protein-protein interaction; Pro, L-proline; PTFE, polytetrafluoroethylene; PTGS2, prostaglandin-endoperoxide synthase 2; QC, quality control; RE, recovery; RPS6KB1, ribosomal protein s6 kinase b1; RSD, relative standard deviation; RT, retention time; S/N, signal/noise; SC, subcutaneous injection; SOD, superoxide dismutase; SPF, specific pathogen free; TTX, tetrodotoxin; UPLC-Q-Orbitrap-HRMS, Ultra-performance liquid chromatography coupled with quadrupole Orbitrap high-resolution mass spectrometry; UPLC-QqQ-MS/MS, ultra-performance liquid chromatography coupled with triple-quadrupole tandem mass spectrometry; VEGFA, vascular endothelial growth factor a; VGSC, voltage-gated sodium channels; VIP, variable important in projection; WB, Western blotting.

Ethics Approval

The experiments were approved by the Ethics Committee of Fujian Medical University (Project Ethics No. FJMU IACUC 2022-0492) in accordance with the guidelines for animal experimentation provided by the National Science and Technology Ethics Committee of China.

Author Contributions

All authors made a significant contribution to the work reported, whether that is in the conception, study design, execution, acquisition of data, analysis and interpretation, or in all these areas; took part in drafting, revising or critically reviewing the article; gave final approval of the version to be published; have agreed on the journal to which the article has been submitted; and agree to be accountable for all aspects of the work.

Funding

This work was supported by the Joint Funds at the Innovation of Science and Technology, Fujian Province, China (No. 2021Y9008), the Project of Young and Middle-Aged Backbone of Fujian Provincial Health Commission, China (No. 2023GGA040).

Disclosure

The authors declare that they have no known competing financial interests or personal relationships that could have appeared to influence the work reported in this paper.

References

1. Knutsen HK, Alexander J, Barregård L, et al. Risks for public health related to the presence of tetrodotoxin (TTX) and TTX analogues in marine bivalves and gastropods. *EFSA J*. 2017;15:4752–4817. doi:10.2903/j.efsa.2017.4752
2. Mariia M, Lukas R, Josef H, et al. Tetrodotoxin: history, biology, and synthesis. *Angew Chem Int Edit*. 2019;58:18338–18387. doi:10.1002/anie.201901564

3. González-Cano R, Ruiz-Cantero MC, Santos-Caballero M, et al. Tetrodotoxin, a potential drug for neuropathic and cancer pain relief. *Toxins*. 2021;13:483–499. doi:10.3390/toxins13070483
4. Bordin P, Dall Ara S, Tartaglione L, et al. First occurrence of tetrodotoxins in bivalve mollusks from Northern Adriatic Sea (Italy). *Food Control*. 2021;120:107510. doi:10.1016/j.foodcont.2020.107510
5. Tinacci L, Malloggi C, Giusti A, et al. Seafood cross-contamination by tetrodotoxin (TTX): management of an unusual route of exposure. *J Consum Prot Food S*. 2024;19:119–122. doi:10.1007/s00003-023-01467-4
6. Zhang Y, Zou S, Yin S, Wang T. Source, ecological function, toxicity and resistance of Tetrodotoxin (TTX) in TTX-bearing organisms: a comprehensive review. *Toxin Rev*. 2023;42:727–740. doi:10.1080/15569543.2023.2253892
7. Xie Z. *National Compendium of Chinese Herbal Medicine*. Beijing, China: People's health publishing house; 1996.
8. Liu R, Wang H, Peng R. Althaea rosea (Linn.) Cavan. flower in the treatment of tetrodotoxin poisoning. *China J Chin Mater Med*. 2001;26:64–65. doi:10.3321/j.issn:1001-5302.2001.04.023
9. Wang X, Zhang H, Cui H. Atagonistic effects of Hollyhock juice to tetrodotoxin. *Chin Gen Pract*. 2010;8:525–526.
10. Wang S, Ju C, Chen M, et al. Combining untargeted and targeted metabolomics to reveal the mechanisms of herb pair Anemarrhena asphodeloides Bunge and Phellodendron chinense C. K. Schneid on benign prostatic hyperplasia. *J Ethnopharmacol*. 2024;334:118539. doi:10.1016/j.jep.2024.118539
11. Guo X, Wu W, Ran Q, et al. Exploring the pharmacological mechanisms of the flower of Rhododendron molle in rheumatoid arthritis rats based on metabolomics integrated network pharmacology. *J Ethnopharmacol*. 2024;334:118524. doi:10.1016/j.jep.2024.118524
12. Wang C, Fu R, Xu D, et al. A study integrated metabolomics and network pharmacology to investigate the effects of Shicao in alleviating acute liver injury. *J Ethnopharmacol*. 2024;319:117369. doi:10.1016/j.jep.2023.117369
13. Wang Y, Zheng R, Wu P, et al. Determination of multiple neurotransmitters through LC-MS/MS to confirm the therapeutic effects of Althaea rosea flower on TTX-intoxicated rats. *Molecules*. 2023;28:4158. doi:10.3390/molecules28104158
14. Patin F, Corcia P, Vourc HP, et al. Omics to explore amyotrophic lateral sclerosis evolution: the central role of arginine and proline metabolism. *mol Neurobiol*. 2017;54:5361–5374. doi:10.1007/s12035-016-0078-x
15. Wang H, Lin J, Xi Y, et al. Clinical experience of combining western medicine with *Althaea rosea* in the treatment of puffer fish poisoning. *J Emerg Tradit Chin Med*. 2000;9(3):2.101–102.
16. Xu Y, Labedan B, Glansdorff N. Surprising arginine biosynthesis: a reappraisal of the enzymology and evolution of the pathway in microorganisms. *Microbiol Mol Biol R*. 2007;71:36–47. doi:10.1128/mmbr.00032-06
17. Buckholtz JW, Meyer-Lindenberg A. MAOA and the neurogenetic architecture of human aggression. *Trends Neurosci*. 2008;31:120–129. doi:10.1016/j.tins.2007.12.006
18. Nagatsu T. Progress in monoamine oxidase (MAO) research in relation to genetic engineering. *Neurotoxicology*. 2004;25:11–20. doi:10.1016/S0161-813X(03)00085-8
19. Van Rhijn J, Shi Y, Bormann M, et al. Brunner syndrome associated MAOA mutations result in NMDAR hyperfunction and increased network activity in human dopaminergic neurons. *Neurobiol Dis*. 2022;163:105587. doi:10.1016/j.nbd.2021.105587
20. Nicholson-Guthrie CS, Guthrie GD, Sutton GP, et al. Urine GABA levels in ovarian cancer patients: elevated GABA in malignancy. *Cancer Lett*. 2001;162:27–30. doi:10.1016/s0304-3835(00)00620-0
21. Curtis RC, Laura AT, Levinus AB, et al. Association between lysine reduction therapies and cognitive outcomes in patients with pyridoxine-dependent epilepsy. *Neurology*. 2022;99:e2627. doi:10.1212/WNL.0000000000201222
22. Minenkova A, Jansen EEW, Cameron J, et al. Is impaired energy production a novel insight into the pathogenesis of pyridoxine-dependent epilepsy due to biallelic variants in ALDH7A1. *PLoS One*. 2021;16:916–923. doi:10.1371/journal.pone.0257073
23. Chen K, Popel AS. Vascular and perivascular nitric oxide release and transport: biochemical pathways of neuronal nitric oxide synthase (NOS1) and endothelial nitric oxide synthase (NOS3). *Free Radical Bio Med*. 2007;42:811–822. doi:10.1016/j.freeradbiomed.2006.12.007
24. Ueda K, Valdivia C, Medeiros-Domingo A, et al. Syntrophin mutation associated with long QT syndrome through activation of the nNOS-SCN5A macromolecular complex. *Proc Natl Acad Sci U S A*. 2008;105:9355–9360. doi:10.1073/pnas.0801294105
25. Scheiblich H, Steinert JR. Nitrergic modulation of neuronal excitability in the mouse hippocampus is mediated via regulation of Kv2 and voltage-gated sodium channels. *Hippocampus*. 2021;31:1020–1038. doi:10.1002/hipo.23366
26. Oliveira JF, Teixeira CE, Arantes EC, et al. Relaxation of rabbit corpus cavernosum by selective activators of voltage-gated sodium channels: role of nitric oxide-cyclic guanosine monophosphate pathway. *Urology*. 2003;62(3):581–588. doi:10.1016/S0090-4295(03)00462-X
27. Pauwels K, Abadjieva A, Hilven P, et al. The N-acetylglutamate synthase/N-acetylglutamate kinase metabolon of Saccharomyces cerevisiae allows co-ordinated feedback regulation of the first two steps in arginine biosynthesis. *Eur J Biochem*. 2003;270:1014–1024. doi:10.1046/j.1432-1033.2003.03477.x
28. Ahern GP, Hsu SF, Klyachko VA, et al. Induction of persistent sodium current by exogenous and endogenous nitric oxide. *J Biol Chem*. 2000;275:28810–28815. doi:10.1074/jbc.M003090200
29. Shi D, Allewell NM, Tuchman M. The N-acetylglutamate synthase family: structures, function and mechanisms. *Int J mol Sci*. 2015;16:13004–13022. doi:10.3390/ijms160613004
30. Yi Z, Lijun J, Qiu C, et al. Hypoglycemic activity evaluation and chemical study on hollyhock flowers. *Fitoterapia*. 2015;102:7–14. doi:10.1016/j.fitote.2015.02.001
31. Tian C, Liu X, Chang Y, et al. Investigation of the anti-inflammatory and antioxidant activities of luteolin, kaempferol, apigenin and quercetin. *S Afr J Bot*. 2021;137:257–264. doi:10.1016/j.sajb.2020.10.022
32. Lesjak M, Beara I, Simin N, et al. Antioxidant and anti-inflammatory activities of quercetin and its derivatives. *J Funct Foods*. 2018;40:68–75. doi:10.1016/j.jff.2017.10.047
33. Marefati N, Ghorani V, Shakeri F, et al. A review of anti-inflammatory, antioxidant, and immunomodulatory effects of Allium cepa and its main constituents. *Pharm Biol*. 2021;59:285–300. doi:10.1080/13880209.2021.1874028
34. Ali F, Rahul, Naz F, et al. Health functionality of apigenin: a review. *Int J Food Prop*. 2017;20:1197–1238. doi:10.1080/10942912.2016.1207188
35. Denaro M, Smeriglio A, Trombetta D. Antioxidant and anti-inflammatory activity of citrus flavanones mix and its stability after in vitro simulated digestion. *Antioxidants-Basel*. 2021;10:140–149. doi:10.3390/antiox10020140